Journal of Power Sources 208 (2012) 120–130

Contents lists available at SciVerse ScienceDirect

Journal of Power Sources

journal homepage: www.elsevier.com/locate/jpowsour

Analysis of an ethanol-fuelled solid oxide fuel cell system using partial anode exhaust gas recirculation

Dang Saebea[a], Yaneeporn Patcharavorachot[a], Amornchai Arpornwichanop[a,b,*]

[a] Department of Chemical Engineering, Faculty of Engineering, Chulalongkorn University, Bangkok 10330, Thailand
[b] Computational Process Engineering, Chulalongkorn University, Bangkok 10330, Thailand

ARTICLE INFO

Article history:
Received 3 December 2011
Received in revised form 5 February 2012
Accepted 7 February 2012
Available online 15 February 2012

Keywords:
Solid oxide fuel cell
Anode exhaust gas recycle
Ethanol reforming
Performance analysis

ABSTRACT

This paper presents an analysis of a solid oxide fuel cell (SOFC) system integrated with an ethanol reforming process. The recycling of the anode exhaust gas in the integrated SOFC system is considered to improve its performance. The results indicate that under the same operating conditions, the SOFC system operated with the recycle of the anode exhaust gas has higher electrical and thermal efficiencies than a non-recycling SOFC system. The required conditions to prevent carbon formation in the ethanol reformer are also examined. When the SOFC system with anode exhaust gas recycling is operated at a higher recirculation ratio and fuel utilization, the carbon formation can be reduced, which in turn decreases the reformer operating temperature. However, the recirculation ratio has to be carefully selected because an increase in the recirculation ratio has an adverse impact on the electrical efficiency of the SOFC system. In addition, the results show that the electrical efficiency depends on the fuel utilization of the SOFC. At low fuel utilization (0.5–0.6), the electrical efficiency increases as the recirculation ratio increases. In contrast, when the SOFC is operated at a higher fuel utilization (>0.6), an increase in the recirculation ratio results in a decrease in the electrical efficiency.

1. Introduction

Fuel cells have been identified as an alternative method to generate power with high efficiency and environmental friendliness when compared to a conventional combustion-based process. Among the various types of fuel cells, the solid oxide fuel cell (SOFC) is the most promising fuel cell technology, as it can be used in a wide range of commercial applications. The high operational temperature of the SOFC (1073–1273 K) results in many advantages; for example, the high-temperature waste heat from a SOFC can be recovered for use in other heat-demanding units in the SOFC system. In addition, different fuels (e.g., methane, methanol, ethanol, etc.) can be directly fed to the SOFC due to the possibility for operation with internal reforming [1].

In general, natural gas is widely used as the fuel for SOFC applications. However, liquid fuels such as ethanol, methanol and gasoline have been recommended for use in automotive applications or auxiliary power units [2–4]. In comparison with other feedstocks, ethanol is considered an economically attractive green fuel as it can be derived renewably from several biomass sources, including energy plants and agriculture residues [5]. In addition, it presents several advantages for fuel cell applications; that is, it has a relatively high hydrogen content and is easy to store, handle and transport safely due to its lower toxicity and volatility [6]. Douvartzides et al. [7] presented a thermodynamic and economic analysis of the electricity generation of SOFCs using various fuels. The results showed that the use of ethanol to produce hydrogen for SOFCs is a very promising option. When ethanol is considered as the primary fuel, it is possible to be internally reformed into a hydrogen-rich gas (synthesis gas) within a fuel cell stack (referred to as an internal reforming SOFC, or IR-SOFC) because the operating temperature of the SOFC is in the same range as that of the reforming reactions. However, it was reported that the direct feed of ethanol to the SOFC stack is not appropriate due to the easy degradation of the Ni/YSZ catalyst at the anode by carbon formation, which leads to the loss of fuel cell performance and poor durability [8]. In order to avoid this problem, the implementation of an external reforming system is a potentially better option because the higher content of hydrogen that is obtained from the conversion of ethanol via a steam reforming process can be introduced to the SOFC stack [9]. Nevertheless, because the steam reforming reaction involves a highly endothermic reaction, the SOFC system with external reforming requires a high external heat source and efficient energy management.

* Corresponding author at: Department of Chemical Engineering, Faculty of Engineering, Chulalongkorn University, Bangkok 10330, Thailand. Tel.: +66 2 218 6878; fax: +66 2 218 6877.
E-mail address: Amornchai.A@chula.ac.th (A. Arpornwichanop).

0378-7753/$ – see front matter © 2012 Elsevier B.V. All rights reserved.
doi:10.1016/j.jpowsour.2012.02.023

Nomenclature

a_c	activity coefficient of carbon
A_c	fuel cell active area (m^2)
$D_{eff,anode}$	effective gaseous diffusivity through anode ($m^2\ s^{-1}$)
$D_{eff,cathode}$	effective oxygen diffusivity through cathode ($m^2\ s^{-1}$)
E^{OCV}	open-circuit voltage (V)
E^0	open-circuit voltage at the standard pressure (V)
E_{anode}	activation energy of anode ($kJ\ mol^{-1}$)
$E_{cathode}$	activation energy of cathode ($kJ\ mol^{-1}$)
F	Faraday constant ($C\ mol^{-1}$)
$\dot{h}$	enthalpy ($kJ\ mol^{-1}$)
ΔH°	standard heat of reaction ($kJ\ mol^{-1}$)
j	current density ($A\ m^{-2}$)
$j_{0,anode}$	exchange current density at anode ($A\ m^{-2}$)
$j_{0,cathode}$	exchange current density at cathode ($A\ m^{-2}$)
k_{anode}	pre-exponential factor of the anode ($A\ m^{-2}$)
$k_{cathode}$	pre-exponential factor of cathode ($A\ m^{-2}$)
K_{eq}	equilibrium constants
$LHV_{C_2H_5OH}$	low heating value of ethanol ($kJ\ s^{-1}$)
n	number of electrons transferred
$\dot{n}$	molar flow rate ($mol\ s^{-1}$)
p_i	partial pressures of component i (bar)
P	operating pressure of SOFC (bar)
P_{sofc}	electrical power output (W)
Q	thermal energy ($kJ\ s^{-1}$)
R	gas constant ($kJ\ mol^{-1}\ K^{-1}$)
R_{ohm}	total internal resistance ($\Omega\ m^2$)
T	temperature (K)
U_f	fuel utilization factor
V	operating cell voltage (V)
$\dot{z}$	amount of hydrogen consumed by the electrochemical reaction ($mol\ s^{-1}$)

Greek symbols

α	transfer coefficient
η	overpotentials (V)
λ_{air}	excess air ratio
σ_{anode}	electronic conductivity of anode ($\Omega^{-1}\ m^{-1}$)
$\sigma_{cathode}$	electronic conductivity of cathode ($\Omega^{-1}\ m^{-1}$)
$\sigma_{electrolyte}$	ionic conductivity of electrolyte ($\Omega^{-1}\ m^{-1}$)
τ_{anode}	thickness of anode (m)
$\tau_{cathode}$	thickness of cathode (m)
$\tau_{electrolyte}$	thickness of electrolyte (m)

Subscripts

a	air channel
conc	concentration overpotentials
f	fuel channel
i	chemical component
j	reaction
ohm	ohmic loss
r	reformer
sofc	solid oxide fuel cell
SM	steam reforming reaction
TPB	three-phase boundary
WGS	water gas shift reaction

When considering the operating parameters of SOFC systems, it has been reported that the fuel utilization is the most important parameter affecting the performance of SOFC. A SOFC operated at high fuel utilization can provide high electrical efficiency. However, at high fuel utilization, more hydrogen is consumed by the electrochemical reactions, and the fuel stream at the SOFC fuel channel is thus diluted by steam [10]. A hydrogen deficiency due to the unbalanced fuel flowing through the SOFC causes a larger buildup of nickel oxide [11] as well as corrosion on the carbon plate [12]. Therefore, it is reasonable to operate the SOFC at a moderate fuel utilization. Under this condition, the SOFC can produce electrical power together with a high-temperature exhaust gas that contains useful remaining fuel (i.e., hydrogen and carbon monoxide). Typically, the exhaust gases from fuel and air channels are burnt in an afterburner to produce more heat, which is used to preheat the fuel stream and supplied to the steam reformer. Although the combustion of exhaust gases can increase the thermal efficiency of the SOFC system, the fuel stream is utilized inefficiently. To improve the overall SOFC performance, a SOFC system with anode exhaust gas recycling has been proposed in the literatures [13–15]. A portion of anode exhaust gas containing useful fuels, i.e., hydrogen and carbon monoxide, is recirculated to mix with the inlet fuel before it is fed to the reformer, whereas the rest of the anode exhaust gas is burnt with the cathode exhaust gas in the afterburner. Interestingly, it is noteworthy that the steam produced by the electrochemical reaction in the anode exhaust gas can be further used as a reagent for steam reforming and thus the requirement for fresh steam can be reduced [16]. Shekhawat et al. [14] demonstrated that the utilization of the anode exhaust gas in the SOFC system integrated with the catalytic partial oxidation of diesel can reduce the carbon formation and increase the hydrogen concentration in the reformate gas. Although the SOFC system with anode exhaust gas recycling was previously studied as mentioned above, there are few studies that investigate in detail the effect of utilizing the anode exhaust gas on the reforming process and the SOFC system performance. This understanding allows for the improvement of the overall SOFC system efficiency.

In this study, the performance of a SOFC system fuelled by synthesis gas derived from an ethanol reforming process with non-recycling and recycling of the anode exhaust gas is investigated based on a thermodynamic analysis. The optimal design of the SOFC system is determined by considering the electrical and thermal efficiencies. In addition, the influences of the fuel utilization and recirculation ratio of the anode exhaust gas on the carbon formation in the ethanol steam reformer and on the system efficiency are investigated to justify the benefit of using the anode exhaust gas recycling.

2. Model of SOFC system

2.1. SOFC system

Fig. 1a and b shows schematics of the ethanol steam reformer and the SOFC integrated system with and without the recycle of the anode exhaust gas, respectively. Both the SOFC systems consist of a vaporizer, heat exchanger, fuel processor, SOFC stack and afterburner. First, ethanol and water are separately fed into the vaporizer and then sent to the heat exchanger to be preheated to the desired operating temperature of the reformer. The ethanol and steam then undergo the steam reforming reaction at the reformer to produce a synthesis gas. The obtained synthesis gas is preheated before being fed to the SOFC stack where the hydrogen in the synthesis gas reacts with oxygen in air to produce electrical power via an electrochemical reaction. The residue fuel in the SOFC outlet stream is combusted in the afterburner and the heat thus generated can be used for the heat-requiring units in the SOFC system. In the case where the anode exhaust gas is recycled (Fig. 1b), a portion of the anode exhaust gas is recycled to the reformer. The steam generated by the electrochemical reaction can be used as

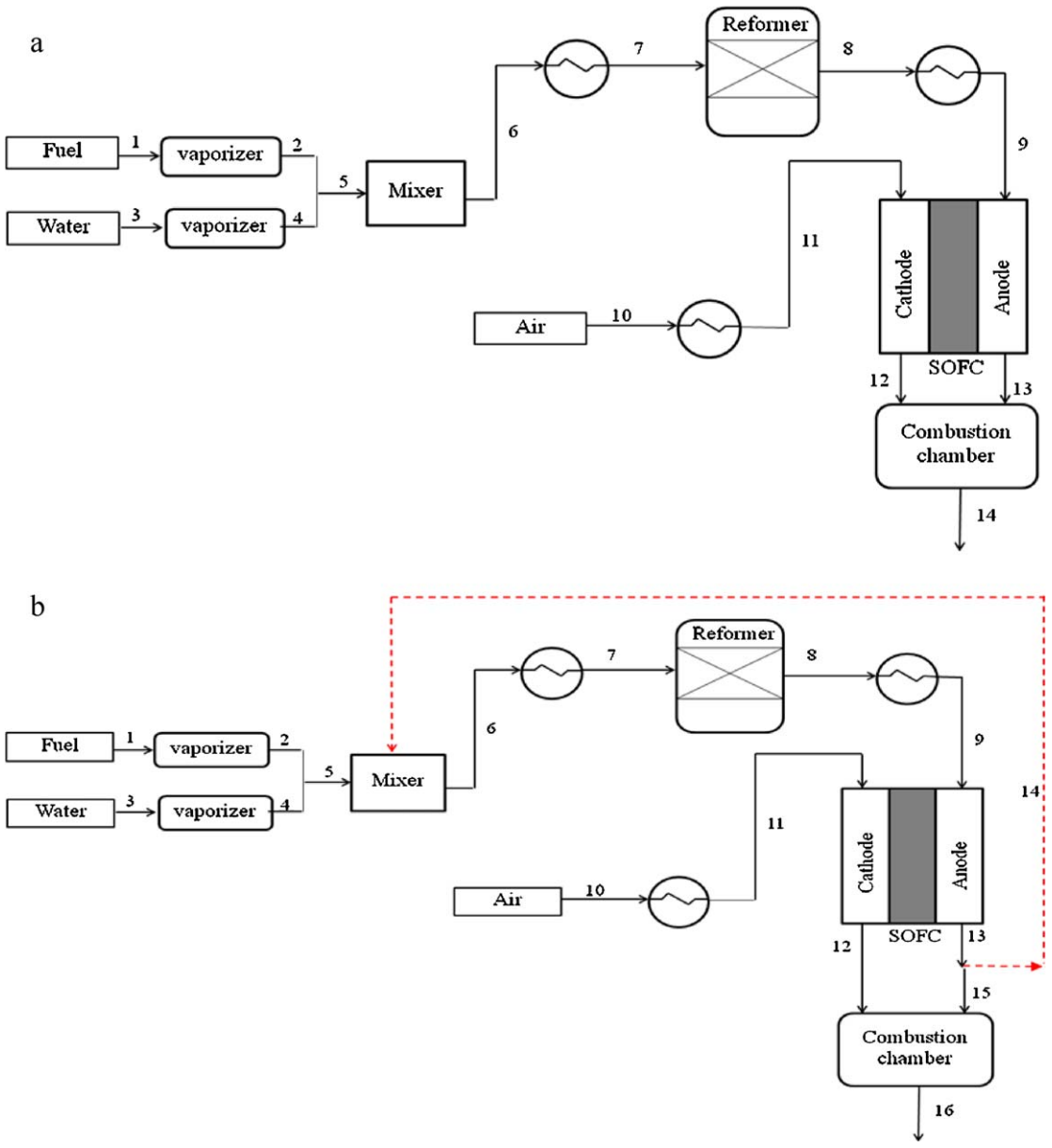

Fig. 1. Schematic of the SOFC systems integrated with an external ethanol steam reformer: (a) no recirculation and (b) anode exhaust gas recirculation.

a reforming reagent, whereas the residue of carbon monoxide in the anode exhaust gas can further react with steam via the water gas-shift reaction to produce more hydrogen in the steam reformer.

The following assumptions have been made for modeling the ethanol steam reforming and SOFC integrated system: (i) heat losses from each unit in the SOFC system are negligible, (ii) all gases behave as ideal gases, and (iii) the temperatures of the system are kept constant.

2.2. Fuel processor

The main reactions that occur in the ethanol steam reformer for hydrogen production are as follows [17]:

$$C_2H_5OH + H_2O \leftrightarrow 4H_2 + 2CO \quad (1)$$

$$CO + H_2O \leftrightarrow H_2 + CO_2 \quad (2)$$

$$CO + 3H_2 \leftrightarrow CH_4 + H_2O \quad (3)$$

The equilibrium composition of the synthesis gas at the outlet of the steam reformer can be determined based on a thermodynamic analysis using a stoichiometric approach. The equilibrium constants of each reaction (Eqs. (1)–(3)) can be written as:

$$K_{eq,SE} = \frac{p_{CO,r}^2 p_{H_2,r}^4}{p_{C_2H_5OH,r} p_{H_2O,r}} \quad (4)$$

$$K_{eq,WGS} = \frac{p_{CO_2,r} p_{H_2,r}}{p_{CO,r} p_{H_2O,r}} \quad (5)$$

$$K_{eq,MR} = \frac{p_{CH_4,r} p_{H_2O,r}}{p_{CO,r} p_{H_2,r}^3} \quad (6)$$

where $K_{eq,j}$ represents the equilibrium constant associated with reaction j and $p_{i,r}$ is the partial pressure of component i in the steam reformer.

The equilibrium constants of all the reactions can be determined by the Van't Hoff equation:

$$\frac{d\ln K}{dT} = \frac{\Delta H^{\circ}}{RT^2} \tag{7}$$

The molar flow rates of each component in the ethanol steam reformer are given by the following expressions:

$$n_{\mathrm{EtOH,r}} = a - x_1 \tag{8}$$

$$n_{\mathrm{H_2O,r}} = b + c - x_1 - x_2 + x_3 \tag{9}$$

$$n_{\mathrm{H_2,r}} = d + 4x_1 + x_2 - 3x_3 \tag{10}$$

$$n_{\mathrm{CO,r}} = g + 2x_1 - x_2 - x_3 \tag{11}$$

$$n_{\mathrm{CH_4,r}} = m + x_3 \tag{12}$$

$$n_{\mathrm{CO_2,r}} = e + x_2 \tag{13}$$

$$n_{\mathrm{total,r}} = \sum_{i-1}^{6} n_i = a + b + c + d + e + g + m + 4x_1 - 2x_3 \tag{14}$$

where x_1, x_2 and x_3 are the extent of reactions of Eqs. (1)–(3) and a and b represent the inlet feed flows of ethanol and water fed to the steam reformer, respectively. When recycling the anode exhaust gas, c, d, e, g and m represent the inlet recycle flows of water, hydrogen, carbon dioxide, carbon monoxide and methane to the steam reformer, respectively.

The following three reactions, i.e., the Boudouard reaction (Eq. (15)), methane cracking (Eq. (16)) and CO reduction (Eq. (17)), are the most probable reactions that can lead to the formation of carbon in the ethanol reforming system:

$$2\mathrm{CO} \leftrightarrow \mathrm{CO_2} + \mathrm{C} \tag{15}$$

$$\mathrm{CH_4} \leftrightarrow 2\mathrm{H_2} + \mathrm{C} \tag{16}$$

$$\mathrm{CO} + \mathrm{H_2} \leftrightarrow \mathrm{H_2O} + \mathrm{C} \tag{17}$$

In this study, the carbon formation is examined by using a thermodynamic analysis that considers the Boudouard reaction because it presents the lowest value of the Gibbs free energy. The possibility of the carbon formation is determined by the value of the carbon activity, defined as:

$$a_{\mathrm{c}} = \frac{K_{\mathrm{b}} p^2_{\mathrm{CO,r}}}{p_{\mathrm{CO_2,r}}} \tag{18}$$

where a_{c} is the activity coefficient of carbon and K_{b} represents the equilibrium constant for the Boudouard reaction. If the carbon activity is greater than unity, the system is not in equilibrium and carbon formation is present. When the carbon activity equals to unity, the system is in equilibrium. Finally, when the carbon activity is less than unity, the formation of carbon is thermodynamically impossible in the system. It is noted that the carbon activity is only the indicator for determining the presence of carbon in the system and thus the amount of carbon formation cannot be examined.

The heat required for the steam reformer operation can be computed from the energy balance equation around the reformer:

$$Q_{\mathrm{SR}} = \left(\sum_{o} \dot{n}_8 \dot{h}_8\right) - \left(\sum_{i} \dot{n}_7 \dot{h}_7\right) \tag{19}$$

2.3. SOFC model

The synthesis gas obtained from the ethanol steam reformer consists of $\mathrm{CH_4}$, $\mathrm{H_2}$, $\mathrm{H_2O}$, CO, and $\mathrm{CO_2}$ and is fed to a fuel channel of the SOFC. Because the SOFC is operated at high temperatures, a steam reforming reaction of methane (Eq. (20)) and a water gas shift reaction (Eq. (21)) can occur within the SOFC stack. Furthermore, the use of Ni-cermet as the anode can provide sufficient activity for the steam reforming reaction.

$$\text{Steam reforming} : \mathrm{CH_4} + \mathrm{H_2O} \leftrightarrow \mathrm{CO} + 3\mathrm{H_2} \tag{20}$$

$$\text{Water gas shift} : \mathrm{CO} + \mathrm{H_2O} \leftrightarrow \mathrm{CO_2} + \mathrm{H_2} \tag{21}$$

Hydrogen is produced from the ethanol steam reformer as well as from the methane reforming and water gas-shift reactions on the anode side and is consumed by the oxidation reaction (Eq. (22)) to generate steam and electrons. Oxygen in the air that is fed at the cathode side is reduced to oxygen ions (Eq. (23)) that migrate through the electrolyte. The overall electrochemical reaction occurring within the SOFC is shown in Eq. (24). The electrons flow from the anode to the cathode to produce direct-current electricity.

$$\text{Anode} : \quad \mathrm{H_2} + \mathrm{O^{2-}} \rightarrow \mathrm{H_2O} + 2\mathrm{e^-} \tag{22}$$

$$\text{Cathode} : \quad 0.5\mathrm{O_2} + 2\mathrm{e^-} \rightarrow \mathrm{O^{2-}} \tag{23}$$

$$\text{Overall reaction} : \quad \mathrm{H_2} + 0.5\mathrm{O_2} \rightarrow \mathrm{H_2O} \tag{24}$$

The molar flow rates of each component at the SOFC outlet can be determined based on the reaction equilibrium. The relationships between the thermodynamic equilibrium constants and gaseous components for the steam reforming and water gas shift reactions in the SOFC stack are shown in Eqs. (25) and (26), respectively.

$$K_{\mathrm{eq,SM}} = \frac{p_{\mathrm{CO,sofc}} p^3_{\mathrm{H_2,sofc}}}{p_{\mathrm{CH_4,sofc}} p_{\mathrm{H_2O,sofc}}} \tag{25}$$

$$K_{\mathrm{eq,WGS}} = \frac{p_{\mathrm{CO_2,sofc}} p_{\mathrm{H_2,sofc}}}{p_{\mathrm{CO,sofc}} p_{\mathrm{H_2O,sofc}}} \tag{26}$$

where $p_{i,\mathrm{sofc}}$ is the partial pressure of species i at the SOFC outlet.

For the SOFC operation, hydrogen is consumed by the electrochemical reaction ($\dot{z}$). The consumption of hydrogen is related to a fuel utilization factor (U_{f}) and the inlet gas compositions, as expressed in Eq. (27).

$$U_{\mathrm{f}} = \frac{\dot{z}}{(4\dot{n}_{\mathrm{CH_4}} + \dot{n}_{\mathrm{H_2}} + \dot{n}_{\mathrm{CO}})} \tag{27}$$

The current density (j) generated by the fuel cell involves the decrease of hydrogen by the electrochemical reaction at the anode side (Eq. (28)):

$$j = \frac{2F\dot{z}}{A_{\mathrm{c}}} \tag{28}$$

where F is the Faraday constant and A_{c} is the fuel cell active area.

The theoretical open-circuit voltage or the reversible cell voltage computed by the difference between the thermodynamic potentials of the electrode reactions can be expressed by the Nernst equation:

$$E^{\mathrm{OCV}} = E^0 - \frac{RT}{2F} \ln\left(\frac{P_{\mathrm{H_2O}}}{P_{\mathrm{H_2}} P^{0.5}_{\mathrm{O_2}}}\right) \tag{29}$$

where E^0 is the open-circuit voltage at standard pressure and is a function of the operating temperature, expressed as:

$$E^0 = 1.253 - 2.4516 \times 10^{-4}\ T \quad (\mathrm{K}) \tag{30}$$

The operating cell voltage or actual fuel cell voltage (V) is always lower than its open-circuit voltage due to the internal voltage losses encountered in real fuel cell operation (Eq. (31)). There are three dominant voltage losses, which are the function of the temperature, current density and substance concentrations.

$$V = E - \eta_{\mathrm{act}} - \eta_{\mathrm{ohm}} - \eta_{\mathrm{conc}} \tag{31}$$

Ohmic losses (η_{ohm}) occur due to the resistance to the flow of ions in the electrolyte and the resistance to the flow of electrons

through the electrodes and current collectors. This loss is linearly correlated with the voltage drop and current density (Eq. (32)).

$$\eta_{ohm} = jR_{ohm} \tag{32}$$

where R_{ohm} is the internal resistance, which depends on the conductivity and thickness of the individual layers as shown below:

$$R_{Ohm} = \frac{\tau_{anode}}{\sigma_{anode}} + \frac{\tau_{electrolyst}}{\sigma_{electrolyst}} + \frac{\tau_{cathode}}{\sigma_{cathode}} \tag{33}$$

where τ_{anode}, $\tau_{cathode}$ and $\tau_{electrolyte}$ are the thickness of the anode, cathode and electrolyte layers, respectively. σ_{anode} and $\sigma_{cathode}$ are the electronic conductivity of the anode and cathode, respectively, and $\sigma_{electrolyte}$ is the ionic conductivity of the electrolyte.

The concentration overpotentials (η_{conc}) are caused by a decrease in the substances at the surface of the electrodes due to the resistance to mass transport. These overpotentials become significant at high current densities because the rate of hydrogen consumption at the reaction sites is higher than that of diffusion of the reactant through the porous electrode to the reaction sites [10,18]. These overpotentials can be expressed as:

$$\eta_{conc} = \eta_{conc,anode} + \eta_{conc,cathode} \tag{34}$$

$$\eta_{conc,anode} = \frac{RT}{2F} \ln\left(\frac{p_{H_2O,TPB} p_{H_2,f}}{p_{H_2O,f} p_{H_2,TPB}}\right) \tag{35}$$

$$\eta_{conc,cathode} = \frac{RT}{4F} \ln\left(\frac{p_{O_2,a}}{p_{O_2,TPB}}\right) \tag{36}$$

The partial pressures of H_2, H_2O, and O_2 at the three-phase boundaries can be determined by using a gas transport model in porous media as shown in the following expressions:

$$p_{H_2,TPB} = p_{H_2,f} - \frac{RT\tau_{anode}}{2FD_{eff,anode}} j \tag{37}$$

$$p_{H_2O,TPB} = p_{H_2O,f} + \frac{RT\tau_{anode}}{2FD_{eff,anode}} j \tag{38}$$

$$p_{O_2,TPB} = P - (P - p_{O_2,a}) \exp\left(\frac{RT\tau_{cathode}}{4FD_{eff,cathode}P} j\right) \tag{39}$$

where P is the operating SOFC pressure, $D_{eff,anode}$ is the effective gaseous diffusivity through the anode (considered to be a binary gas mixture of H_2 and H_2O) and $D_{eff,cathode}$ is the effective oxygen diffusivity through the cathode (considered to be a binary gas mixture of O_2 and N_2).

The activation overpotentials (η_{act}) are caused by the sluggishness of the electrochemical reaction at the electrode surfaces. The activation overpotentials can be determined by the non-linear Butler–Volmer equation as follows:

$$j = j_{0,anode}\left[\frac{p_{H_2,TPB}}{p_{H_2,f}} \exp\left(\frac{\alpha nF}{RT}\eta_{act,anode}\right) - \frac{p_{H_2O,TPB}}{p_{H_2O,f}} \exp\left(-\frac{(1-\alpha)nF}{RT}\eta_{act,anode}\right)\right] \tag{40}$$

$$j = j_{0,cathode}\left[\exp\left(\frac{\alpha nF}{RT}\eta_{act,cathode}\right) - \exp\left(-\frac{(1-\alpha)nF}{RT}\eta_{act,cathode}\right)\right] \tag{41}$$

where α is the transfer coefficient (usually considered to be 0.5), n is the number of electrons transferred in the single elementary rate-limiting reaction step represented by the Butler–Volmer equation and $j_{0,cathode}$ and $j_{0,anode}$ are the exchange current density at the cathode and the anode, which depend on the operating temperature as shown in Eqs. (42) and (43), respectively.

$$j_{0,cathode} = \frac{RT}{nF} k_{cathode} \exp\left(-\frac{E_{cathode}}{RT}\right) \tag{42}$$

$$j_{0,anode} = \frac{RT}{nF} k_{anode} \exp\left(-\frac{E_{anode}}{RT}\right) \tag{43}$$

where $E_{cathode}$ and E_{anode} represent the activation energies at the anode and the cathode, which are equal to 137 and 140 kJ mol^{-1}, respectively, and $k_{cathode}$ and k_{anode} denote the pre-exponential factors, which are 2.35×10^{11} and 6.54×10^{11} Ω^{-1} m^{-2}, respectively [10].

The electrical power output (P_{sofc}) is obtained when a current is drawn from the fuel cell, defined as:

$$P_{sofc} = I \times V_{actual} = j \times V_{actual} \times A_c \tag{44}$$

where V_{actual} represents the actual voltage and I is the current flowing through the fuel cell.

In this study, the SOFC is operated under adiabatic condition; therefore, the air flowing through the SOFC is employed to control the fuel cell temperature. The air inlet temperature can be calculated from the energy balance around the fuel cell, given as:

$$\left(\sum_i \dot{n}_9 \dot{h}_9\right) + \left(\sum_i \dot{n}_{11} \dot{h}_{11}\right) - \left(\sum_o \dot{n}_{12} \dot{h}_{12}\right) - \left(\sum_o \dot{n}_{13} \dot{h}_{13}\right) - P_{sofc} = 0 \tag{45}$$

2.4. Other units

2.4.1. Vaporizers

Ethanol and water are converted from the liquid to the gas phase in the vaporizer. The required heat for the operation of the vaporizer can be expressed as:

$$Q_{vap,C_2H_5OH} = \left(\sum_o \dot{n}_2 \dot{h}_2\right) - \left(\sum_i \dot{n}_1 \dot{h}_1\right) \tag{46}$$

$$Q_{vap,H_2O} = \left(\sum_o \dot{n}_4 \dot{h}_4\right) - \left(\sum_i \dot{n}_3 \dot{h}_3\right) \tag{47}$$

2.4.2. Pre-heaters

As seen in Fig. 1, the SOFC system has three pre-heaters that are used to preheat the feed stream of ethanol and steam, the synthesis gas obtained from the reformer and the air fed to the SOFC. The heat required for these pre-heaters can be determined by the following equations:

$$Q_{preheater,1} = \left(\sum_o \dot{n}_7 \dot{h}_7\right) - \left(\sum_i \dot{n}_6 \dot{h}_6\right) \tag{48}$$

$$Q_{preheater,2} = \left(\sum_o \dot{n}_9 \dot{h}_9\right) - \left(\sum_i \dot{n}_8 \dot{h}_8\right) \tag{49}$$

$$Q_{preheater,3} = \left(\sum_o \dot{n}_{11} \dot{h}_{11}\right) - \left(\sum_i \dot{n}_{10} \dot{h}_{10}\right) \tag{50}$$

2.4.3. Mixer

For the SOFC system with anode exhaust gas recycling, the recirculated gas stream is mixed with the fresh fuel feed in a mixer. The

Table 1
Values of the structural parameters for the planar SOFC.

Cell length, L (m)	0.4
Cell width, W (m)	0.1
Fuel channel height, h_f (mm)	1
Air channel height, h_a (mm)	1
Anode thickness, τ_{anode} (μm)	500
Cathode thickness, $\tau_{cathode}$ (μm)	50
Electrolyte thickness, $\tau_{electrolyte}$ (μm)	20

outlet temperature of the mixer can be calculated from the energy balance around the mixer, expressed as:

$$\left(\sum_i \dot{n}_5\dot{h}_5\right) + \left(\sum_i \dot{n}_{14}\dot{h}_{14}\right) - \left(\sum_o \dot{n}_6\dot{h}_6\right) = 0 \quad (51)$$

2.4.4. After-burner

The residue flue gas from the anode outlet stream and the unused oxidant gas from the cathode are mixed and burnt in an afterburner. The combustion reactions that occur in the afterburner can be written as follows:

$$\text{Hydrogen combustion}: \quad H_2 + 0.5O_2 \rightarrow H_2O \quad (52)$$

$$\text{Carbon monoxide combustion}: \quad CO + 0.5O_2 \rightarrow CO_2 \quad (53)$$

For the non-recycling SOFC system, the exit temperature of the afterburner can be calculated from the energy balance on the afterburner as:

$$\left(\sum_i \dot{n}_{12}\dot{h}_{12}\right) + \left(\sum_i \dot{n}_{13}\dot{h}_{13}\right) - \left(\sum_o \dot{n}_{14}\dot{h}_{14}\right) = 0 \quad (54)$$

For the SOFC system with anode exhaust gas recycling, the portion of the anode flue gas that is not recycled to the reformer is fed into the afterburner. The exit temperature of the afterburner outlet is calculated by solving the following equation:

$$\left(\sum_i \dot{n}_{12}\dot{h}_{12}\right) + \left(\sum_i \dot{n}_{15}\dot{h}_{15}\right) - \left(\sum_o \dot{n}_{16}\dot{h}_{16}\right) = 0 \quad (55)$$

The performance parameters of the SOFC system are considered in terms of the electrical efficiency (η_{el}) and the thermal efficiency (η_{th}), which are defined as:

$$\eta_{el} = \frac{P_{sofc}}{\dot{n}_{C_2H_5OH} LHV_{C_2H_5OH}} \quad (56)$$

$$\eta_{th} = \frac{Q_{rec} - Q_{use}}{\dot{n}_{C_2H_5OH} LHV_{C_2H_5OH}} \quad (57)$$

where $\dot{n}_{C_2H_5OH}$ is the inlet ethanol molar flow rate, $LHV_{C_2H_5OH}$ is the lower heating value of ethanol, Q_{rec} is the thermal energy obtained from the SOFC system (the reference temperature is 100 °C) and Q_{use} is the total thermal energy used in the SOFC system.

2.5. Solution approach

The performance of the SOFC system with non-recycling and recycling of the anode exhaust gas is analyzed based on the SOFC system model mentioned in the previous section. The proposed model consists of a set of nonlinear algebraic equations and was coded and solved by using MATLAB. Tables 1–3 list the parameters of the SOFC geometry, material properties and operating conditions for the SOFC system under nominal conditions [1,10,18]. The SOFC model was verified with the experimental data of Zhao and Virkar [19] to ensure its reliability. The values of the operating parameters used for model validation are presented in Table 4. The comparison of the model prediction with the experimental data regarding the operating voltage of the SOFC at different current densities and operating temperatures is shown in Fig. 2. It can be seen that the model prediction shows a good agreement with the experimental data of the SOFC operated under the temperature range used in this study. The model parameters may differ from the experiment as they are taken from different sources and this factor causes the error between the model prediction and experimental data; however, this error can be reasonably acceptable.

For the simulations of the SOFC system with anode exhaust gas recycling, an iterative approach is employed: the recycle stream (i.e., the composition of the anode exhaust gas) is assumed to be variable and the SOFC system model is solved until the assumed variables are recalculated. This procedure is repeated until the difference in the values of the assumed and calculated variables satisfies a desired accuracy (10^{-6}).

Table 2
Values of the kinetic and material property parameters for the SOFC.

Pre-exponential factor of anode exchange current density, k_{anode} (A m^{-2})	6.54×10^{11}
Pre-exponential factor of cathode exchange current density, $k_{cathode}$ (A m^{-2})	2.35×10^{11}
Activation energy of anode exchange current density, E_{anode} (kJ mol^{-1})	140
Activation energy of cathode exchange current density, $E_{cathode}$ (kJ mol^{-1})	137
Anode diffusion coefficient, $D_{eff,anode}$ (m^2 s^{-1})	3.66×10^{-5}
Cathode diffusion coefficient, $D_{eff,cathode}$ (m^2 s^{-1})	1.37×10^{-5}
Anode electrical conductivity, σ_{anode} (Ω^{-1} m^{-1})	$\frac{4.2\times10^7}{T} \exp\left(\frac{-1200}{T}\right)$
Cathode electrical conductivity, $\sigma_{cathode}$ (Ω^{-1} m^{-1})	$\frac{9.5\times10^7}{T} \exp\left(\frac{-1150}{T}\right)$
Electrolyte ionic conductivity, $\sigma_{electrolyte}$ (Ω^{-1} m^{-1})	$33.4 \times 10^3 \exp\left(\frac{-10300}{T}\right)$

Table 3
Values of the operating conditions for the SOFC system under nominal conditions.

Pre-reformer unit	
Operating temperature, T_r (K)	973 K
Operating pressure, P_r (bar)	1
Molar flow of ethanol (mol s^{-1})	1
Solid oxide fuel cell unit	
Operating temperature, T_{sofc} (K)	1073
Operating pressure, P_{sofc} (bar)	1
Air composition	21% O_2, 79% N_2
Fuel utilization	0.7
Excess air ratio	8.5
SOFC pressure drop (%)	2

Table 4
Values of the input parameters used in the model validation [19].

Operating temperature, T_{sofc} (K)	873, 973, 1073
Operating pressure, P_{sofc} (bar)	1
Air composition	21% O_2, 79% N_2
Fuel composition	97% H_2, 3% H_2O
Cell dimensions	
Cell length, L (m)	0.4
Cell width, W (m)	0.1
Fuel channel height, h_f (mm)	1
Air channel height, h_a (mm)	1
Anode thickness, τ_{anode} (μm)	1000
Cathode thickness, $\tau_{cathode}$ (μm)	20
Electrolyte thickness, $\tau_{electrolyte}$ (μm)	8

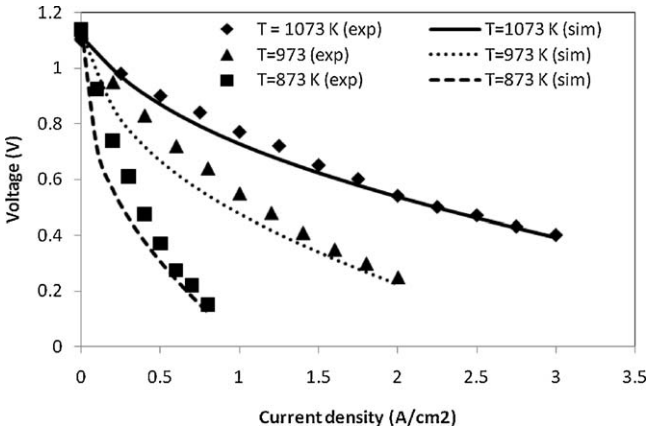

Fig. 2. Comparison between the model predictions and experimental results of Zhao and Virkar [19].

3. Results and discussion

3.1. Comparison of SOFC systems with and without anode exhaust gas recycling

The performances of the SOFC system with and without recycling the anode exhaust gas are first analyzed under nominal conditions. The steam and ethanol fed to the ethanol steam reformer are fixed at the ratio of 1.5. The results show that the electrical performance of the SOFC system with the anode gas recycling is 46.16%, which is higher than that without the anode gas recycle (42.87%). Table 4 shows the heat duty needed in each unit of both SOFC systems. The energy requirements for the ethanol processor section of the SOFC system with and without the anode exhaust gas recirculation are 397.10 and 634.18 kW, respectively. The recirculation of the anode gas reduces the energy required by the fuel processor (37.4% reduction). In addition, it is observed that all of the steam required for the steam reformer is recovered by the anode exhaust gas recirculation (the recirculation ratio = 0.6), and this can save the energy supplied to the water vaporizer. However, the total energy requirements of the two SOFC systems are not different. The SOFC with anode gas recirculation can produce more electrical power and thus requires a high air supply to maintain the temperature of the SOFC. This results in high energy consumption in the air pre-heater. It is noted that since the power required to drive the blower for the anode exhaust gas recycling has slight effect on the SOFC system, it is negligible in calculating the electrical efficiency of the SOFC system.

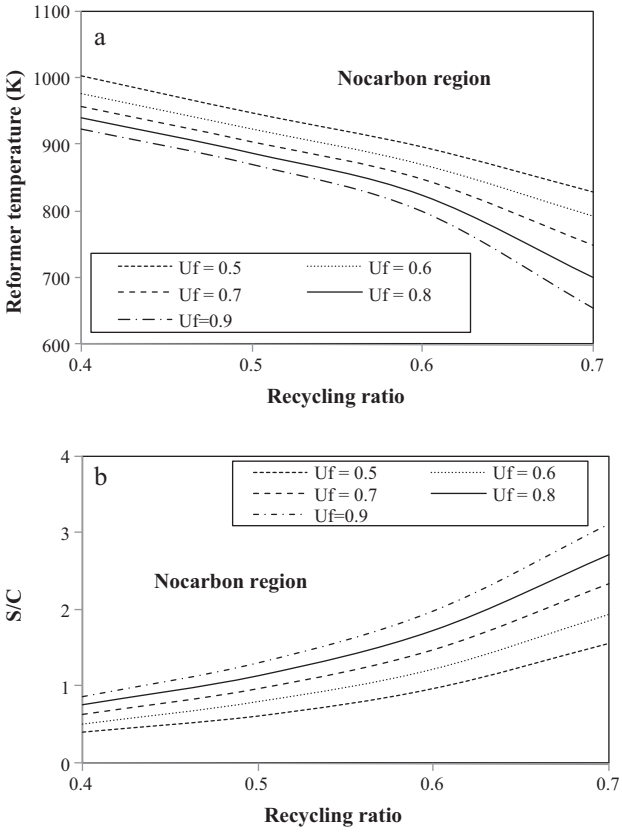

Fig. 4. Effect of the recirculation ratio of the anode exhaust gas at different fuel utilizations on the requirement of (a) the reformer temperature and (b) the steam-to-carbon ratio, to avoid a carbon formation.

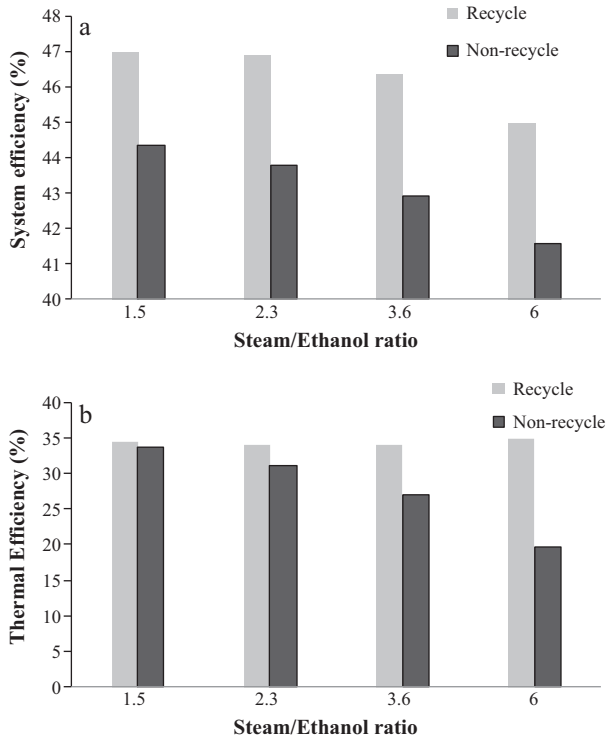

Fig. 3. Performance of the SOFC systems with and without recycling the anode exhaust gas at different steam-to-ethanol ratios: (a) electrical efficiency and (b) thermal efficiency.

Fig. 3 shows a comparison of the SOFC system performance when not recycling and recycling the anode exhaust gas at different steam-to-ethanol feed ratios. The simulation results clearly show that the SOFC system with anode exhaust gas recycling provides higher electrical and thermal efficiencies than that without recycling the anode exhaust gas. In the case of the SOFC system with anode exhaust gas recirculation, it is found that the molar flow rates of hydrogen and carbon monoxide in the SOFC feed stream increase. As a result, the current density generated by the SOFC is more produced, resulting in higher electrical and thermal efficiencies.

Considering the effect of the steam-to-ethanol feed ratio, the electrical performance of both SOFC systems decreases when increasing the steam-to-ethanol feed ratio. This can be explained by a dilution of the hydrogen fed to the SOFC. Unlike the electrical efficiency, when more steam is added, the thermal efficiency of the SOFC system operated with a recycle of the anode exhaust gas slightly increases because the load of steam generation is reduced.

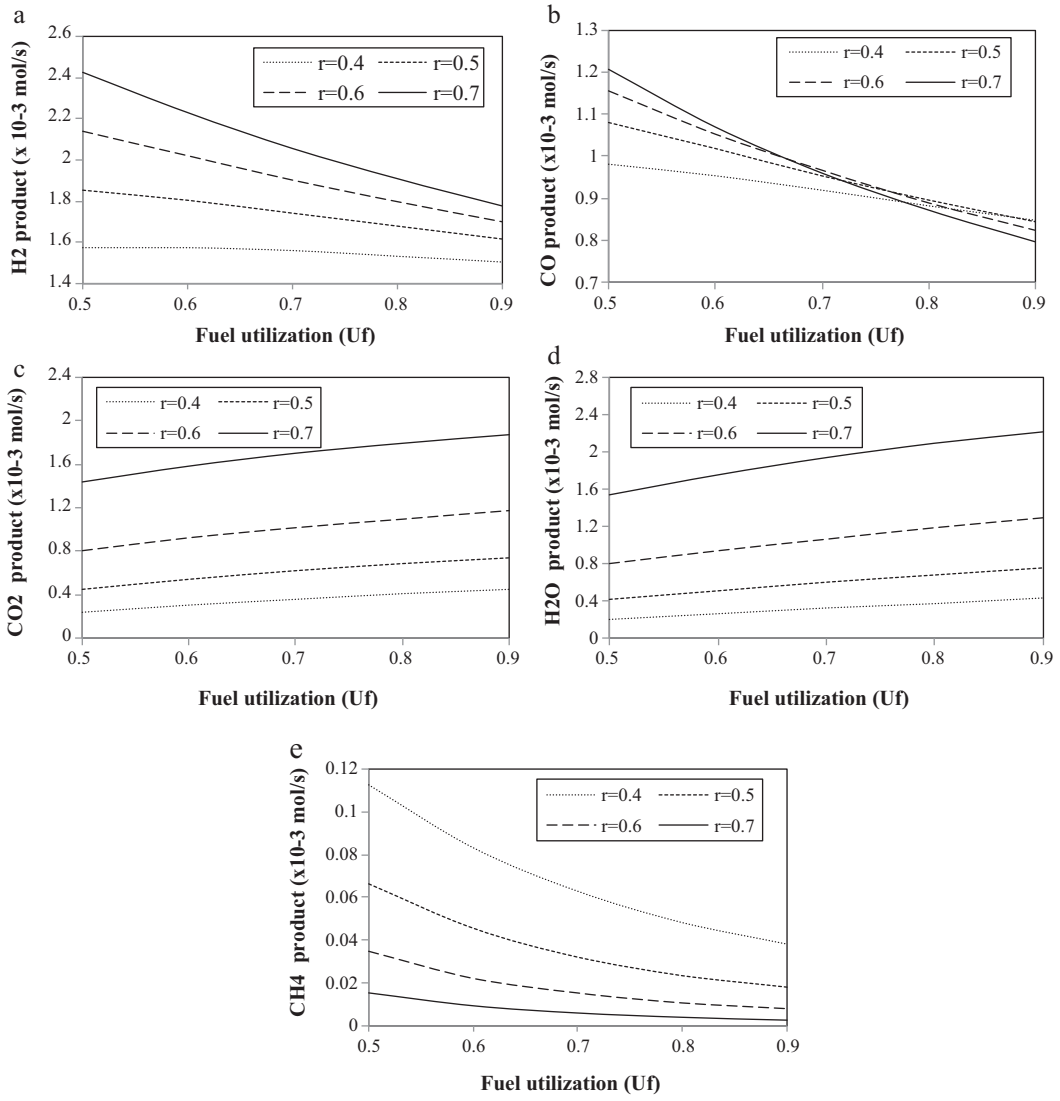

Fig. 5. Effect of fuel utilization on the composition of the synthesis gas obtained from the ethanol steam reformer at different recirculation ratios.

In addition, the high-temperature recycling gas reduces the external heat load for the SOFC feed pre-heater. In contrast, for the conventional SOFC system, an increase in the steam-to-ethanol ratio leads to a higher energy requirement for evaporating and preheating feed the steam, and thus the thermal efficiency is significantly decreased.

3.2. Effects of recirculation ratio and fuel utilization

It is well known that a crucial problem of ethanol steam reforming is caused by the formation of carbon (graphite), which could lead to the deactivation of the catalyst and increased pressure drops in the reformer. To avoid carbon formation, the suitable operating temperature and steam-to-carbon ratio should be determined. In general, a steam reforming reaction needs to be fed with excess steam to increase hydrogen production and to reduce the carbon monoxide. The presence of carbon monoxide will promote carbon formation via the Boudouard reaction (Eq. (15)). Furthermore, the tendency of carbon formation decreases as the reforming temperature increases due to the exothermic nature of the Boudouard reaction. However, operation of the steam reformer at a high temperature with more steam addition results in a high operating cost (Table 5).

Fig. 4 presents the effect of the recirculation ratio of the anode exhaust gas on the reformer temperature and steam-to-carbon ratio required to avoid carbon formation at different fuel utilizations. It is noted that the fuel utilization affects the gaseous composition of the residual gas exiting from the SOFC anode, whereas the recirculation ratio indicates the amount of the steam,

Table 5
Heat duty of each unit in the SOFC systems with and without anode exhaust gas recirculation.

Heat exchangers	Heat duty (kW)	
	SOFC system without recycling the anode-exhaust gas	SOFC system with recycling the anode-exhaust gas
Ethanol vaporizer	49.12	49.12
Water vaporizer	167.88	–
Pre-heating gas before reformer	152.04	33.18
Pre-heating gas before SOFC	30.44	47.61
Reformer	234.70	267.19
Air pre-heater	1503.94	1731.53
Total	2138.1	2128.63

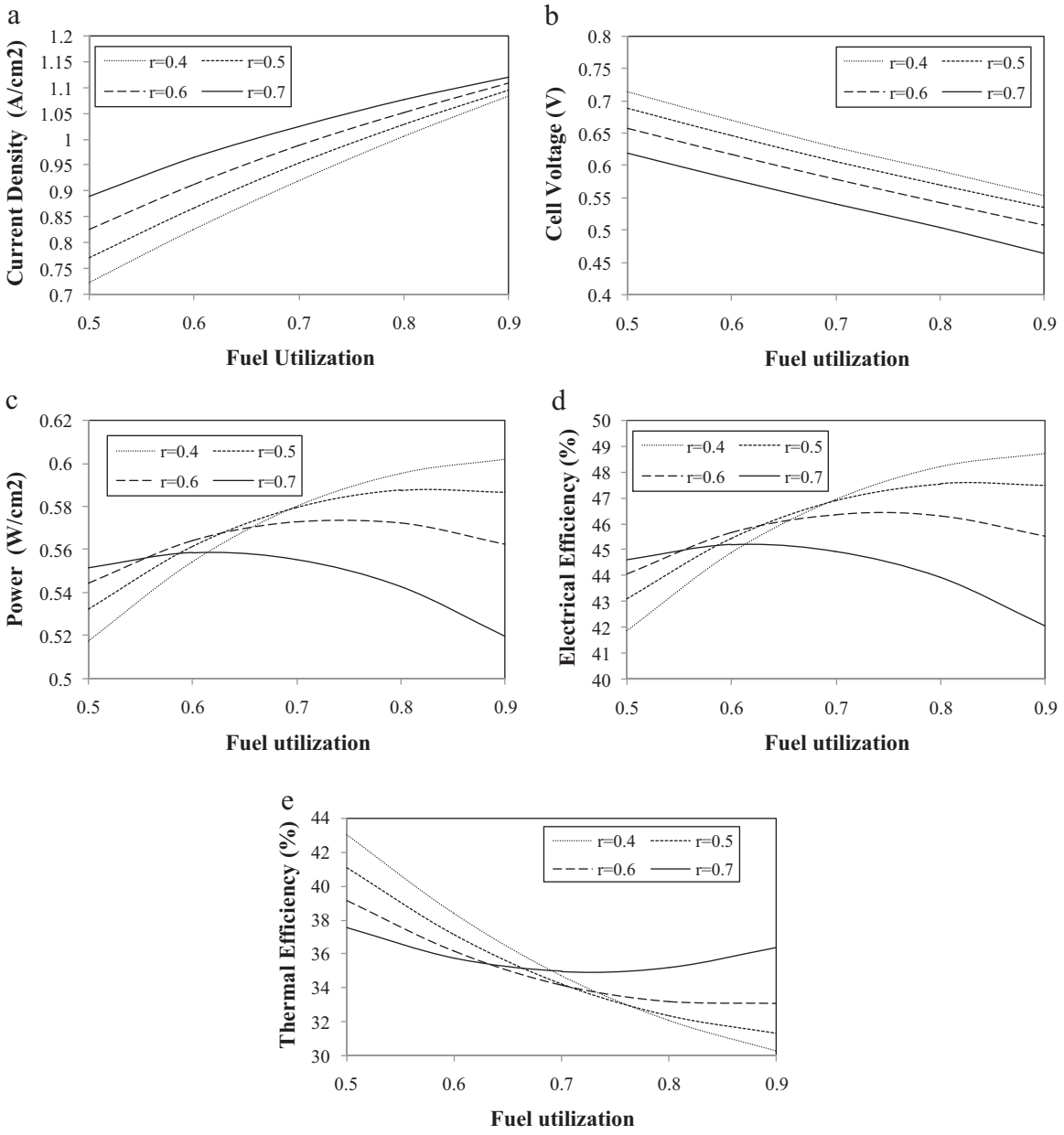

Fig. 6. Effect of fuel utilization on the SOFC system performance at different recirculation ratios: (a) current density, (b) fuel cell voltage, (c) power density, (d) electrical efficiency, and (e) thermal efficiency.

which is generated by the electrochemical reaction, that is recycled to the ethanol steam reforming section.

As seen in Fig. 4a, the reforming temperature required to suppress the tendency of carbon formation is reduced when the SOFC is operated at the higher recirculation ratio and fuel utilization. The higher recirculation ratio increases the recycle of the steam to the ethanol reformer. Furthermore, at high fuel utilization, more steam is also generated from the SOFC stack. These factors lead to an increase in the steam-to-carbon ratio of the reformer feed (Fig. 4b). From the simulation result, when the SOFC system with anode exhaust gas recycling is operated at a low fuel utilization of 0.6 and recirculation ratio of 0.4, the reforming temperature should be higher than 970 K to prevent the formation of carbon in the ethanol reformer.

Fig. 5a–e shows the molar flow rates of hydrogen, carbon monoxide, carbon dioxide, steam and methane at the outlet of the ethanol reformer as functions of the recirculation ratio and fuel utilization. As expected, the amount of hydrogen and carbon monoxide decreases as the fuel utilization of the SOFC increases, whereas carbon dioxide and steam increase because the electrochemical and water gas shift reactions in the SOFC are more pronounced. The results show that an increase in the recirculation ratio increases the flow rates of the steam, carbon dioxide, carbon monoxide and hydrogen. However, at high fuel utilization, the carbon monoxide flow rate decreases when the recirculation ratio increases. At these conditions, more steam is recycled to the reformer, promoting the water gas shift reaction. It is noted that when the SOFC is operated at a high fuel utilization and recirculation ratio, a higher steam content in the anode exhaust gas and also a decrease in the content of methane at the reformer outlet is observed due to an increase in the reverse methanation reaction.

The influences of the fuel utilization and recirculation ratio on the current density, cell voltage, power density and electrical and

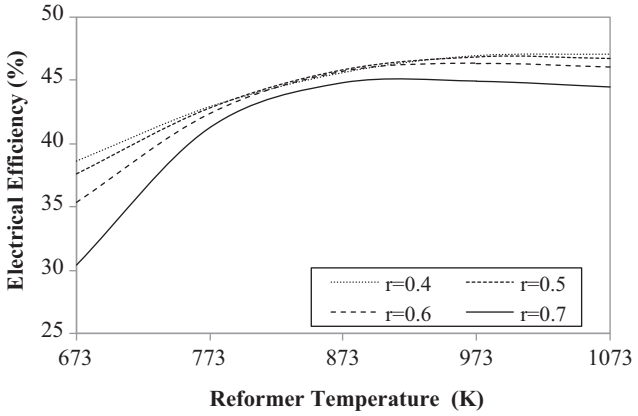

Fig. 7. Effect of the reformer operating temperature on the electrical efficiency of the SOFC system at different recirculation ratios.

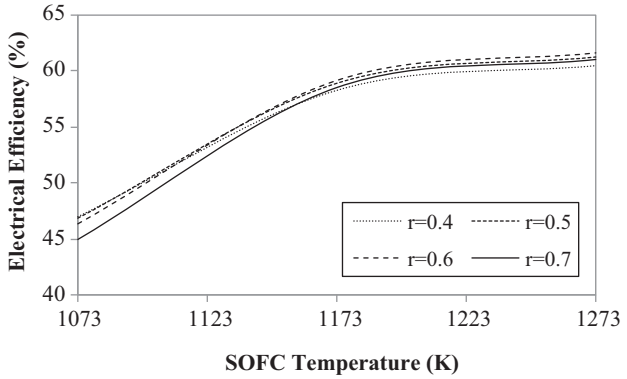

Fig. 8. Effect of the SOFC operating temperature on the electrical efficiency of the SOFC system at different recirculation ratios.

thermal efficiencies are shown in Fig. 6. It can be seen that increasing the fuel utilization and the recirculation ratio cause the SOFC to generate more current density (Fig. 6a). When the SOFC is operated at higher fuel utilization, more hydrogen is consumed to produce electricity, while increasing the recirculation ratio of the anode exhaust gas leads to an increase in the molar flow rate of fuel to the SOFC. However, it is found that the operating cell voltage decreases with the increments of fuel utilization and recirculation ratio (Fig. 6b). This is mainly due to a significant increase of steam in the anode exhaust gas as the fuel utilization and recirculation ratio increase. Although a higher amount of steam promotes the ethanol reforming reaction, an excess of steam results in a dilution of the hydrogen required for the electrochemical reaction. This leads to a significant decrease in the open-circuit voltage and an increase in the concentration loss.

Fig. 6c and d shows that at low fuel utilization (0.5–0.6), the power density and electrical efficiency of SOFC increase with the increasing recirculation ratio. As the anode exhaust gas consists of a higher unreacted fuel content due to the low fuel utilization, an increase in the recirculation ratio results in an increase in hydrogen at the SOFC anode inlet, improving the SOFC performance in terms of current density, power density and electrical efficiency. However, the power density and the SOFC electrical efficiency decrease when increasing the recirculation ratio at high fuel utilization. Even though an increase in the fuel utilization results in more current density generated, the increased recirculation ratio causes a significant decrease in the fuel cell voltage. This implies that at high fuel utilization, the decrease in the fuel cell voltage has a strong impact on the power density and electrical efficiency, compared with an increase in the current density.

Considering the thermal efficiency of the SOFC system (Fig. 6e), when the SOFC is operated at low fuel utilization, an increase in the recirculation ratio decreases the thermal efficiency. Operation of the SOFC at a high recirculation ratio lowers the amount of the exhaust gas sent to the afterburner; therefore, the heat generated from the afterburner for use in the SOFC system will decrease. However, the thermal efficiency can be enhanced when the SOFC system is operated at a higher recirculation ratio and higher fuel utilization. This is mainly because the significant increase of steam recycled to the ethanol reformer reduces the demand of energy for generating steam and preheating fuel stream.

3.3. Effects of reformer and SOFC operating temperature

The effect of the reformer temperatures on the electrical efficiency when the SOFC is operated at temperature of 1073 K is shown in Fig. 7. The electrical efficiency of the SOFC system with the anode gas recirculation considerably increases when increasing the reformer temperature. As the ethanol steam reforming is favored in operation at high temperatures, the increase in produced hydrogen promotes the electrochemical reaction in the SOFC stack, and thus, the electrical efficiency of SOFC is enhanced. However, an increase in the recirculation ratio results in a lower SOFC electrical efficiency. The degradation of the SOFC performance is obviously noticed when the reformer is operated at unsuitable temperatures. This lowers the production of hydrogen fuel for the SOFC. In addition, at a high recirculation of the anode exhaust gas, more steam is added to the SOFC, thereby decreasing the fuel cell voltage and the electrical efficiency.

Fig. 8 presents the electrical efficiency of the SOFC system as a function of the SOFC operating temperatures when the reformer is

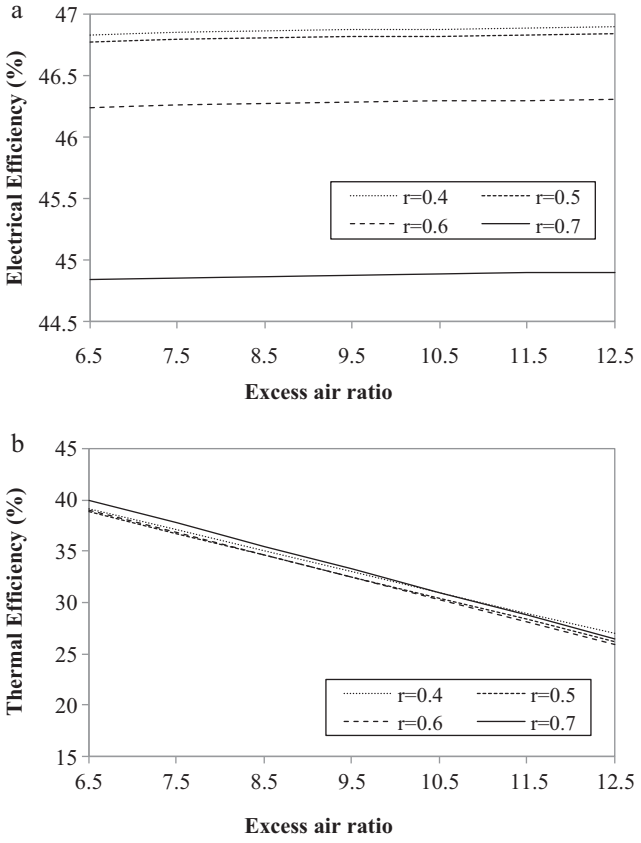

Fig. 9. Effect of the excess air ratio on (a) the electrical efficiency and (b) the thermal efficiency of the SOFC system at different recirculation ratios.

operated at temperature of 973 K. It can be seen that the electrical efficiency increases as the operating temperature of SOFC increases. An increase in the SOFC operating temperature can improve its performance because the rate of the electrochemical reaction is more pronounced. In addition, at elevated temperatures, the ohmic and activation losses are also reduced. Therefore, the more current density is generated, leading to the increased electrical efficiency.

3.4. Effect of excess air ratio

The influence of the excess air ratio on the system's electrical and thermal efficiencies at different recirculation ratios is presented in Fig. 9a and b, respectively. The excess air ratio has a slight effect on the system electrical efficiency but a larger effect on the system thermal efficiency. The thermal efficiency sharply drops when the SOFC system is operated at a high excess air ratio owing to an increased requirement of the heat duty of the air pre-heater.

4. Conclusions

The performance analysis of a SOFC system fuelled by ethanol is presented in this work. An electrochemical model of the SOFC and an equilibrium model of ethanol steam reforming are employed to simulate the SOFC system. The performance of two SOFC systems with and without anode exhaust gas recirculation is compared. The results indicate that the SOFC system with anode exhaust gas recycling provides higher electrical and thermal efficiencies than that of a non-recycling SOFC system. It is found that the tendency of carbon formation in the ethanol steam reformer decreases with an increasing recirculation ratio and fuel utilization in the SOFC stack. At low fuel utilization, the electrical efficiency of the SOFC system increases with the increasing recirculation ratio while the thermal efficiency decreases. The performances of the SOFC system show an opposite trend at high fuel utilization operation. Therefore, the recirculation ratio must be carefully selected. Furthermore, the electrical efficiency of the SOFC system can be enhanced when the ethanol reformer and SOFC stack are operated at high temperatures.

Acknowledgements

Support from the Thailand Research Fund and the Higher Education Research Promotion and National Research University Project of Thailand, Office of the Higher Education Commission (EN280A) is gratefully acknowledged.

D. Saebea would like to thank the Office of the Higher Education Commission, Thailand for their grant support under the program "Strategic Scholarships for Frontier Research Network for the Joint Ph.D. Program Thai Doctoral degree" for this research.

References

[1] Y. Patcharavorachot, W. Paengjuntuek, S. Assabumrungrat, A. Arpornwichanop, Int. J. Hydrogen Energy 35 (2010) 4301–4310.
[2] A. Perna, Int. J. Hydrogen Energy 32 (2007) 1811–1819.
[3] M. Santin, A. Traverso, L. Magistri, Appl. Energy 86 (2009) 2204–2212.
[4] M.D. Falco, Fuel 90 (2011) 739–747.
[5] J. Comas, F. Marino, M. Laborde, N. Amadeo, Chem. Eng. J. 98 (2004) 61–68.
[6] L.E. Arteaga, L.M. Peralta, V. Kafarov, Y. Casas, E. Gonzales, Chem. Eng. J. 136 (2008) 256–266.
[7] S.L. Douvartzides, F.A. Coutelieris, P.E. Tsiakaras, J. Power Sources 114 (2003) 203–212.
[8] N. Laosiripojana, S. Assabumrungrat, J. Power Sources 163 (2007) 943–951.
[9] D. Cocco, V. Tola, Energy 34 (2008) 2124–2130.
[10] P. Aguiar, C.S. Adjiman, N.P. Brandon, J. Power Sources 138 (2004) 120–136.
[11] P. Nehter, J. Power Sources 164 (2007) 252–259.
[12] H. Nishikawa, H. Sasou, R. Kurihara, S. Nakamura, A. Kano, K. Tanaka, T. Aoki, Y. Ogami, Int. J. Hydrogen Energy 33 (2008) 6262–6269.
[13] M. Granovskii, I. Dincer, M.A. Rosen, J. Power Sources 165 (2007) 307–314.
[14] D. Shekhawat, D.A. Berry, T.H. Gardner, D.J. Haynes, J.J. Spivey, J. Power Sources 168 (2007) 447–483.
[15] K. Onda, T. Iwanari, N. Miyauchi, K. Ito, T. Ohba, Y. Sakaki, S. Nagata, J. Electrochem. Soc. 150 (2003) A1569–A1576.
[16] R. Peter, R. Dahl, U. Kluttgen, C. Plam, D. Stolten, J. Power Sources 106 (2002) 238–244.
[17] S. Freni, G. Maggio, S. Cavallaro, J. Power Sources 62 (1996) 67–73.
[18] Y. Patcharavorachot, A. Arpornwichanop, A. Chuachuensuk, J. Power Sources 177 (2008) 254–261.
[19] F. Zhao, A.F. Virkar, J. Power Sources 141 (2005) 79–95.